A Method for Parameter Extraction and Channel State Prediction in Mobile-to-Mobile Wireless Channels

RAMONI ADEOGUN
School of Engineering and Computer Science,Victoria University of Wellington
Wellington
NEW ZEALAND
ramoni.o.adeogun@ieee.org

Abstract: This paper investigates the prediction of single input single output (SISO) narrowband multipath fading channels for mobile-to-mobile wireless communications. Using a statistical model for mobile to mobile urban and suburban channels, we derive a parametrized model and utilize the ESPRIT algorithm to extract the effective Doppler frequencies from noisy channel estimates. The parameter estimates are then used to forecast the mobile-to-mobile channel into the future. Using the Cramer Rao bound for function of parameters, a bound on the prediction error of M2M wireless channels is derived. Simulations were performed to evaluate the performance of the prediction scheme and comparison was made with the prediction of typical fixed to mobile channels and also with the derived bound. Results show that the performance of the scheme approaches the bound as the SNR increases.

Key–Words: Multipath fading channels, mobile-to-mobile channel, parameter estimation, ESPRIT, channel estimation and prediction.

1 Introduction

Mobile-to-mobile (M2M) land wireless communication channels arise when the transmitter and receiver are moving and are both equipped with low elevation antenna elements. For instance, a moving vehicle in a given location might communication with one or more mobile vehicles in other locations. These systems have several potential applications in traffic safety, rescue squads communication, congestion avoidance, etc. Recently, an international wireless standard, IEEE 802.11p, also referred to as Wireless Access in Vehicular Environment (WAVE) has been developed. Based on the WiFi technology, this standard is proposed for both mobile to mobile and mobile to infrastructure traffic applications.

In order to cope with the challenge of developing and evaluating the performance of current and future mobile to mobile wireless communication systems, several research results have been published on the modelling of single input single output (SISO) mobile- to-mobile channels. In [1, 2], the statistical properties of narrowband SISO mobile to mobile multipath fading channel was investigated based on models for the channel impulse response and transfer function. The authors of [3] present results on the temporal correlation properties and Doppler power spectral characteristics in 3D propagation environments. These results have shown that the fading and statistics of mobile to mobile channel differ significantly from classical fixed to mobile channel where the transmitter is stationary.

In this paper, we investigate the prediction of SISO mobile to mobile channel fading channels. It is well known from channel prediction studies for fixed to mobile channels [4, 5, 6] that channel prediction offer significant benefit in mitigating against performance loss from multipath fading and improving the system performance by providing both the transmitter and receiver with accurate forecast of the channel impulse response. We believed that this fact, coupled with the faster variation exhibited by mobile to mobile channels, make channel prediction an important technique for mobile-to mobile channels. Based on statistical model of the narrowband mobile to mobile channel, we derive a model to estimate the effective Doppler frequencies using super resolution subspace based Estimation of Signal parameters via Rotational Invariance Techniques (ESPRIT) algorithm and applying the parameters estimates for predicting the fading mobile to mobile channel impulse response. A similar approach based on two-dimensional ESPRIT have been presented in [7] for wideband mobile-to-mobile systems. The Cramer Rao bound on the prediction of mobile to mobile channels is also derived.

The rest of this paper is organized as follows. In Section 2, we present the statistical channel model for mobile to mobile channel and derive a simple parametrized model for parameter estimation and prediction. In Section 3, we describe the ESPRIT based approach for estimating the effective Doppler frequency along with the least square amplitude estimation. In Section 4, we present the parametric prediction based on the estimated parameters. The performance bound on the prediction of mobile-to-mobile channels is derived in Section 5. Section 6 present some results from the numerical simulations. Finally, conclusions are drawn in Section 7.

2 Channel Models

This section present the Rayleigh fading narrowband SISO M2M channel considered in this paper along with a reduced parametrized model for mobile to mobile parameter estimation and prediction.

2.1 Mobile-to-Mobile Channel Model

We consider a SISO mobile to mobile wireless communication system. Fig. 1 shows an illustration of the mobile to mobile propagation in typical urban and suburban environments. Both the transmitter and receiver are assumed to be moving with velocities V_T and V_R, respectively. It is further assumed that both the transmitter and receiver are equipped with low elevation omnidirectional antennas. As shown in Fig. 1, a signal will arrive at the receiver via scattering and reflection in all directions, by local scatterers/reflectors around the transmitter and receiver and all distant scattering mediums. It is also assumed that the line-of-sight (LOS) component is obstructed by obstacles between the transmitter and receiver. The complex Rayleigh faded channel is thus modelled as [1, 2]

$$h(t) = \sum_{k=1}^{K} \alpha_k \exp(j[(\omega_{Tk} + \omega_{Rk})t + \phi_k]) \tag{1}$$

where α_k is the Rayleigh distributed amplitude for the kth path, ϕ_k is the kth path phase parameter assumed to be uniformly distributed on $(0, 2\pi)$ and K is the number of propagation paths. ω_{Tk} and ω_{Rk} are the radian Doppler shifts resulting for the mobility of the transmitter and receiver, respectively and are given by

$$\omega_{Tk} = \frac{2\pi}{\lambda} V_T \cos(\theta_{Tk}) \tag{2}$$

$$\omega_{Rk} = \frac{2\pi}{\lambda} V_R \cos(\theta_{Rk}) \tag{3}$$

where θ_{Tk} and θ_{Rk} are random angles of departure at the transmitter and angles of arrival of the kth path respectively. λ is the carrier wavelength. As can be seen from (1), the receive signal will experience Doppler frequency

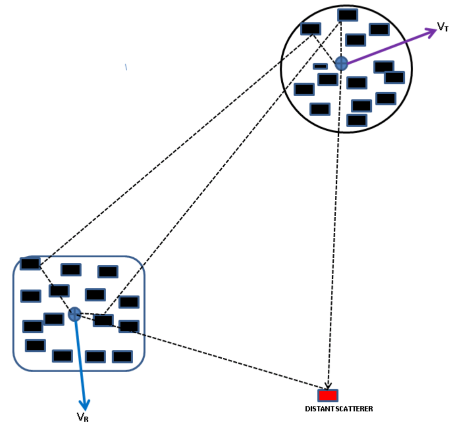

Figure 1: Mobile-to-mobile propagation environment.

shifts due to the mobility of both the transmitter and receiver. The dual mobility in mobile to mobile channels result in more rapid temporal variation of the fading envelope when compared with classical mobile cellular system with fixed transmitter. It should be noted that the sum of sinusoids model commonly used for SISO prediction studies (see e.g [8, 5, 9, 10]) is a special case of (1) with $V_T = 0$.

2.2 Parametrized Model

In order to reduce the mobile-to-mobile channel prediction problem to a sinusoidal parameter estimation problem, we denote

$$\beta_k = \alpha_k \exp(j\phi_k) \tag{4}$$

and

$$\begin{aligned} \omega_k &= \omega_{Tk} + \omega_{Rk} \\ &= \frac{2\pi}{\lambda}(V_T \cos(\theta_{Tk}) + V_R \cos(\theta_{Rk})) \end{aligned} \tag{5}$$

We will henceforth, refer to β_k as the complex amplitude of the kth path and ω_k as the effective radian Doppler frequency. Substituting (4) and (5) into (1), we obtain

$$h(t) = \sum_{k=1}^{K} \beta_k \exp(j\omega_k t) \tag{6}$$

The parameters β_k and ω_k are assumed constant over the region of interest.We also assumed that L samples of the channel are known either by transmitting known pilot sequences or from measurement. In practice, the estimated or measured channel will be imperfect due to the effects of noise and multiuser interference. We therefore model the known channel at time t as

$$\hat{h}(t) = h(t) + z(t) \tag{7}$$

where $h(t)$ is the actual channel and $z(t)$ is a random variable that accounts for the effect of noise and interference. For simplicity reasons, we assume that $z(t)$ is zero mean Gaussian with variance σ_z^2.

3 Parameter Acquisition

In this section, we present the method for estimating the Doppler frequencies and complex amplitudes of the mobile-to-mobile channel. Due to its high resolution and low complexity, the Doppler estimation stage is based on the ESPRIT (Estimation of Signal Parameters via Rotational Invariance Techniques) algorithm.

3.1 Doppler Frequency Estimation

Assuming that the sampling interval is Δt, the L known samples of the channel can be expressed in vector form using (5) and (6) as

$$\hat{\mathbf{h}} = \mathbf{F}\boldsymbol{\beta} + \mathbf{z} \tag{8}$$

where

$$\hat{\mathbf{h}} = \begin{bmatrix} \hat{h}(0) \\ \hat{h}(\Delta t) \\ \vdots \\ \hat{h}((L-1)\Delta t) \end{bmatrix} \in \mathbb{C}^{L\times 1}, \tag{9}$$

$$\mathbf{F} = \begin{bmatrix} 1 & 1 & \cdots & 1 \\ f_1 & f_2 & \cdots & f_K \\ \vdots & \vdots & \ddots & \vdots \\ f_1^{L-1} & f_2^{L-1} & \cdots & f_K^{L-1} \end{bmatrix} \in \mathbb{C}^{L\times K}, \tag{10}$$

and

$$\boldsymbol{\beta} = [\beta_1, \beta_2, \cdots, \beta_K]^T \tag{11}$$

$[\cdot]$ denotes the transpose operation. $f_k = \exp(j\omega_k \Delta t)$ and $\mathbf{z} \in \mathbb{C}^{L\times 1}$ is the noise vector. Letting F_{UP} and F_{DOWN} be the matrix F without the bottom and top rows respectively, we can form the following equation

$$\mathbf{F}_{UP}\boldsymbol{\gamma} = \mathbf{F}_{DOWN} \tag{12}$$

where

$$\boldsymbol{\gamma} = \begin{bmatrix} f_1 & 0 & \cdots & 0 \\ 0 & f_1 & \cdots & 0 \\ \vdots & \vdots & \ddots & \vdots \\ 0 & 0 & \cdots & f_K \end{bmatrix} \in \mathbb{K}\times\mathbb{K} \tag{13}$$

Assuming that $\mathbf{F}$ is known, (13) for the effective Doppler frequencies. However, $\mathbf{F}$ is unknown in practice but span the signal subspace. We form an Hankel matrix from (8) as

$$\hat{\mathbf{H}} = \begin{bmatrix} \hat{h}(0) & \hat{h}(\Delta t) & \cdots & \hat{h}((P-1)\Delta t) \\ \hat{h}(\Delta t) & \hat{h}(2\Delta t) & \cdots & \hat{h}(P\Delta t) \\ \vdots & \vdots & \ddots & \vdots \\ \hat{h}((Q-1)\Delta t) & \hat{h}(Q\Delta t) & \cdots & \hat{h}((L-1)\Delta t) \end{bmatrix} \tag{14}$$

where $P+Q = L+1$. The size of the H is essentially limited by the number of samples in the training segment. The choice of the Hankel size parameters is thus a compromise between accuracy, identifiability and complexity. In order to have a sufficiently large correlation matrix, we compute P in this paper using[1]

$$P = \lceil \frac{2}{3} L \rceil \tag{15}$$

where $\lceil A \rceil$ denotes the smallest integer greater than A. The temporal correlation is then obtained as

$$\hat{\mathbf{R}} = \frac{\hat{\mathbf{H}}\hat{\mathbf{H}}^\dagger}{P} \tag{16}$$

where $\dagger$ denotes Hermitian transpose.

The signal subspace matrix can be obtained from the singular value decomposition (SVD) or eigen value decomposition (EVD) of $\hat{\mathbf{R}}$. Based on the estimated eigenvalues, the number of dominant paths is estimated using the Minimum Description length (MDL) criterion [12, 13]. Once K is estimated, the signal subspace matrix $\hat{\mathbf{V}}_s$ is obtained from the $\hat{K}$ eigenvectors corresponding to the largest eigenvalues of $\hat{\mathbf{R}}$. Similar to (15), we form the following invariance equation

$$\hat{\mathbf{V}}_{sUP}\boldsymbol{\Phi} = \hat{\mathbf{V}}_{sDOWN} \tag{17}$$

where $\boldsymbol{\Phi}$ is a subspace rotated version of $\boldsymbol{\gamma}$. It has been shown that $\boldsymbol{\Phi}$ and $\boldsymbol{\gamma}$ have common eigenvalues [14] which are used to estimate the Doppler frequencies. Equation (17) can be solved in the least square sense to obtain

$$\boldsymbol{\Phi} = (\hat{\mathbf{V}}_{sUP}^\dagger \hat{\mathbf{V}}_{sUP})^{-1} \hat{\mathbf{V}}_{sUP}^\dagger \hat{\mathbf{V}}_{sDOWN} \tag{18}$$

The effective Doppler radian Doppler frequencies are given as

$$\hat{\omega}_k = \frac{\arg(\lambda_k)}{\Delta t} \tag{19}$$

where λ_k is the kth eigenvalue of $\boldsymbol{\Phi}$ and $\arg(\cdot)$ denotes the phase angle of the associated complex number on $(0, 2\pi]$.

[1] Note that this is a rule of thumb for the choice of Hankel size parameter as given in [11]. The choice of P is essentially a compromise between complexity of the algorithm and accuracy of the correlation estimates.

3.2 Complex Amplitude Estimation

Once the effective Doppler frequencies have been estimated, the complex amplitudes of the dominant paths are computed via a solution of the set of linear equations in (9). We solve the equations using regularized least squares as

$$\hat{\boldsymbol{\beta}} = (\mathbf{F}^\dagger \mathbf{F} + \nu \mathbf{I})^{-1} \mathbf{F}^\dagger \hat{\mathbf{h}} \tag{20}$$

where ν is a regularization parameter that is introduced to minimize the effects of errors in $\mathbf{F}$ on the predictor performance.

4 Channel Estimation and Prediction

Using the estimated parameters, the mobile to mobile channel impulse response can be extrapolated into the future by substituting the parameters into (5) for the desired time instant. The predicted channel is given by

$$\tilde{h}(\tau) = \sum_{k=1}^{\hat{K}} \hat{\beta}_k \exp(j\hat{\omega}_k \tau); \quad \forall \tau = L\Delta t, (L+1)\Delta t, \cdots \tag{21}$$

5 Cramer Rao Bound

In the previous section, we present a scheme for estimating the Doppler frequency and complex amplitudes and predicting the mobile to mobile channel. This section presents a derivation of the lower bound on the parameter estimation and prediction error in SISO mobile to mobile wireless channels. Our derivations will be based on a sampled version of (6) defined as

$$h(\ell) = \sum_{k=1}^{K} \beta_k \exp(j\ell\Delta t \omega_k) \quad \ell = 0, \cdots, L-1 \tag{22}$$

For convenience, we arrange the L observations into the $L \times 1$ vector

$$\mathbf{h} = \begin{bmatrix} h(0) \\ h(1) \\ h(2) \\ \vdots \\ h(L-1) \end{bmatrix} = \begin{bmatrix} \sum_{k=1}^{K} \beta_k \\ \sum_{k=1}^{K} \beta_k \exp(j\Delta t \omega_k) \\ \sum_{k=1}^{K} \beta_k \exp(j2\Delta t \omega_k) \\ \vdots \\ \sum_{k=1}^{K} \beta_k \exp(j(L-1)\Delta t \omega_k) \end{bmatrix} \tag{23}$$

which can be compactly expressed as

$$\begin{aligned} \mathbf{h} &= \sum_{k=1}^{K} \mathbf{f}_k \beta_k \\ &= \mathbf{F}\boldsymbol{\beta} \end{aligned} \tag{24}$$

Note that $\mathbf{F}$ can be expressed as

$$\mathbf{F} = [\mathbf{f}_1 \quad \mathbf{f}_2 \quad \cdots \quad \mathbf{f}_K] \tag{25}$$

where

$$\mathbf{f}_k = [1 \quad \exp(j\Delta t \omega_k) \quad \cdots \quad \exp(j(L-1)\Delta t \omega_k)]^T \tag{26}$$

Let the parametrization of the channel be

$$\boldsymbol{\theta} = [\Re[\boldsymbol{\beta}] \quad \Im[\boldsymbol{\beta}] \quad \boldsymbol{\omega}] \tag{27}$$

The prediction error at the lth time instant is given by

$$\begin{aligned} e(l) &= h(l;\boldsymbol{\theta}) - h(l;\hat{\boldsymbol{\theta}}) \\ &= \sum_{k=1}^{K} \beta_k \exp(j\ell\Delta t \omega_k) - \sum_{k=1}^{\hat{K}} \hat{\beta}_k \exp(j\ell\Delta t \hat{\omega}_k) \end{aligned} \tag{28}$$

Since the channel model is a nonlinear function of the multipath parameters, the prediction error (PE) can be bounded by the Cramer Rao lower bound for function of parameters as

$$\begin{aligned} \mathrm{PE}(\ell) &= (h(l;\boldsymbol{\theta}) - h(l;\hat{\boldsymbol{\theta}}))(h(l;\boldsymbol{\theta}) - h(l;\hat{\boldsymbol{\theta}}))^\dagger \\ &\geq \frac{\partial h(\ell)}{\partial \boldsymbol{\theta}} \mathbf{J}(\boldsymbol{\theta})^{-1} \frac{\partial h(\ell)}{\partial \boldsymbol{\theta}}^\dagger \end{aligned} \tag{29}$$

where $\mathbf{J}^{-1}(\boldsymbol{\theta})$ is the inverse of the Fisher information matrix (FIM) and the lower bound on the variance of the parameter estimates. The Jacobian in (29) is defined as

$$\frac{\partial h(\ell)}{\partial \boldsymbol{\theta}} = \left[\frac{\partial h(\ell)}{\partial \Re[\boldsymbol{\theta}]} \quad \frac{\partial h(\ell)}{\partial \Im[\boldsymbol{\theta}]} \quad \frac{\partial h(\ell)}{\partial \boldsymbol{\omega}} \right] \tag{30}$$

The FIM can be found using the Bangs formula as [15]

$$\mathbf{J}(\boldsymbol{\theta}) = \frac{2}{\sigma^2} \Re \left[\frac{\partial h(\ell)}{\partial \boldsymbol{\theta}}^\dagger \frac{\partial h(\ell)}{\partial \boldsymbol{\theta}} \right] \tag{31}$$

where we have assumed that the noise in the available channel estimates is Gaussian with variance σ^2 and that the noise covariance is independent of the channel parameters. Clearly, the bound on the parameters estimates can be found by evaluating the derivatives in (30) and (31). Using (24), the derivatives with respect to each of the parameter vectors in (27) are obtained as

$$\begin{aligned} \frac{\partial \mathbf{h}}{\partial \Re(\boldsymbol{\beta})} &= \mathbf{F} \\ \frac{\partial \mathbf{h}}{\partial \Im(\boldsymbol{\beta})} &= j\mathbf{F} \\ \frac{\partial \mathbf{h}}{\partial \boldsymbol{\omega}} &= \mathbf{D}_f \mathbf{Y} \end{aligned} \tag{32}$$

Table 1: Simulation Parameters

Parameter	Value
Carrier Frequency	2.0 GHz
Transmitter Velocity	5 Kmph
Training Length	$30-70$
Receiver Velocity	50 Kmph
Angle of Departure	$\mathbb{U}[-\pi,\pi]$
Angle of Arrival	$\mathbb{U}[-\pi,\pi)$
Sampling Interval	1 ms
Number of Paths	5 - 30
Amplitude	$\mathbb{N}(0,1)$
Phase	$\mathbb{U}(0,2\pi)$

where $\mathbf{Y} = \mathrm{diag}[\boldsymbol{\beta}]$ and $\mathbf{D}_f$ is denoted as

$$\mathbf{D}_f = \left[\frac{\mathrm{d}\mathbf{f}_1}{\mathrm{d}\omega_1} \quad \frac{\mathrm{d}\mathbf{f}_2}{\mathrm{d}\omega_2} \quad \cdots \frac{\mathrm{d}\mathbf{f}_K}{\mathrm{d}\omega_K}\right] \tag{33}$$

Substituting (32) into (30) gives

$$\frac{\partial h(\ell)}{\partial \boldsymbol{\theta}} = [\mathbf{F} \quad j\mathbf{F} \quad \mathbf{D}_f\mathbf{Y}] \tag{34}$$

Let $\mathbf{X}_1$ and $\mathbf{X}_2$ be defined as

$$\begin{aligned} \mathbf{X}_1 &= [\mathbf{1} \quad j\mathbf{1} \quad \boldsymbol{\beta}] \\ \mathbf{X}_2 &= [\mathbf{F} \quad \mathbf{F} \quad \mathbf{D}_f] \end{aligned} \tag{35}$$

Using the formulation in (35), it can be easily shown that (34) reduces to

$$\frac{\partial h(\ell)}{\partial \boldsymbol{\theta}} = \mathbf{X}_1 \diamond \mathbf{X}_2 \tag{36}$$

where $\diamond$ is the Khatri-Rao product. The FIM is thus

$$\mathbf{J}(\boldsymbol{\theta}) = (\mathbf{X}_1 \diamond \mathbf{X}_2)^\dagger (\mathbf{X}_1 \diamond \mathbf{X}_2) \tag{37}$$

Once the FIM have been evaluated using (37), the error bound can be found by substituting into (29).

6 Numerical Simulations

In this section, we analyze the performance of the mobile to mobile parametric channel prediction algorithm and compare with the prediction of fixed to mobile channel with equal receiver velocity and stationary transmitter [11]. Comparison is also made with the Cramer Rao bound.

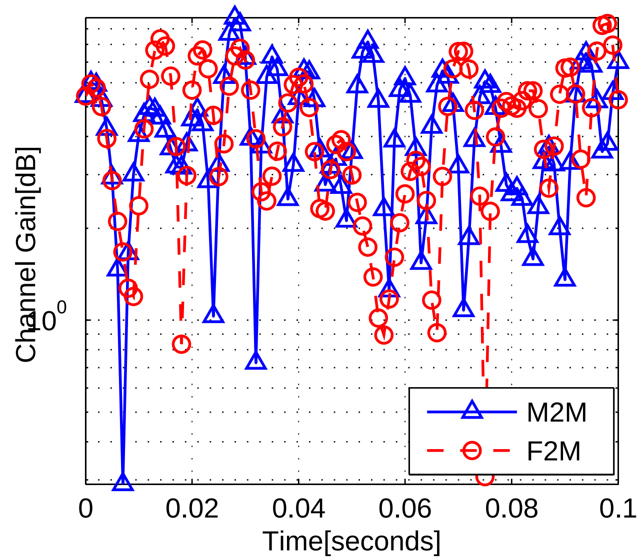

Figure 2: Amplitude of Mobile to Mobile (M2M) and Fixed to Mobile (F2M) Channel versus Time.

6.1 Performance Comparison

The prediction error of the algorithms is evaluated using the normalized mean squared error (NMSE) criterion

$$\begin{aligned} \mathrm{NMSE}(\tau) &= \frac{\mathbb{E}[|\tilde{h}(\tau) - h(\tau)|^2]}{\mathbb{E}[|h(\tau)|^2]} \\ &\approx \frac{1}{M}\sum_{m=1}^{M} \frac{\sum_{z=1}^{Z} |\hat{h}(\tau) - h(\tau)|^2}{\sum_{z=1}^{Z} |h(\tau)|^2} \end{aligned} \tag{38}$$

where M is the number of snapshots. The channel is generated using the parameters in Table 1 (except where otherwise stated). In Figure 2, we present a snapshot of the amplitude of mobile to mobile channel and fixed to mobile channel impulses responses as a function of time. As can be seen from the figure, the temporal variation of the mobile to mobile channel is relatively faster when compared with the fixed to mobile. This is possibly due to the dual mobility. This agreed with observations in [1, 2] where it was also shown that mobile to mobile channels has significantly different statistics. Figure 3 shows the normalized mean square error (NMSE) versus prediction horizon. As expected, the NMSE increases with increasing prediction horizon and decreases with increasing signal to noise ratio (SNR). We observe no significant different in NMSE for the prediction of M2M and F2M channel at all time instants considered. It should however be noted that the prediction horizon measured in unit of time corresponds to different spatial distance for the two channels depending on the mobile velocities and direction of motion. In Figure 4, we present the cumulative distribution function (CDF) of

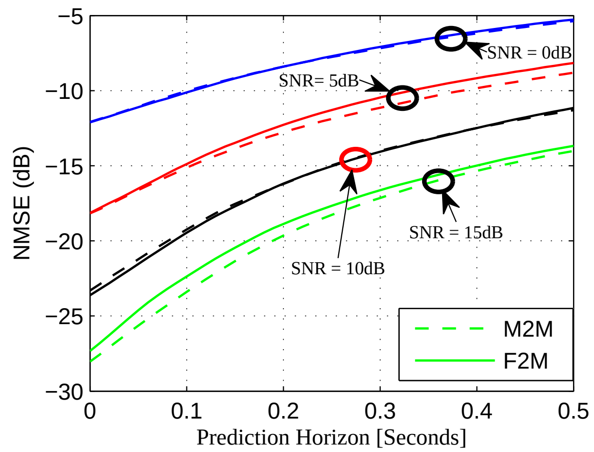

Figure 3: NMSE versus prediction horizon for M2M and F2M channel prediction at different SNR.

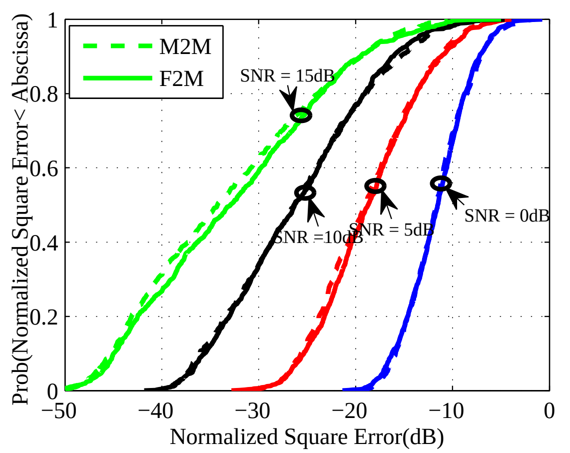

Figure 4: The CDF of NSE for a prediction horizon of $100\,ms$ at $\mathrm{SNR} = 10\,\mathrm{dB}$ using 50 samples in the training segment.

normalized square error for a prediction horizon of $100\,ms$ at $\mathrm{SNR} = 10\,dB$. Figure 5 shows the NMSE as a function of prediction horizon with different number of propagation paths in the channel. As shown in the figure, increasing the number of paths increases the prediction error. However, as the number of of paths increases, the rate of increase of the error decreases. For instance, an increase of about $8\,dB$ in NMSE results from increasing the number of paths from 5 to 10 and the increase was just about 1 dB when for an increase from 25 to 30 paths. Finally, we show the CDF of normalized square error with different number of samples in the training segment at an SNR of 10 dB in Fig. 6. It shows that increasing the training length improves the prediction performance.

6.2 Comparison with Prediction Error Bound

We here compare the performance of the M2M prediction scheme presented in this paper with the derived error bound. Figure 7 presents the prediction error and error bound versus SNR for a prediction horizon of $0.05\,ms$. It shows that the performance of the algorithm approaches the bound with increasing SNR. This is expected since the ESPRIT algorithm [14] upon which the prediction is based has been shown to be an asymptotic maximum likelihood parameter estimator.

7 Conclusion

In this paper, we performed a detailed investigation on the prediction of single input single output (SISO) mobile-to-mobile wireless communication channels. Starting with a statistical model for M2M channels, we derive a model for estimating the effective Doppler frequency shifts via an ESPRIT-type algorithm. Simulation results show that mobile-to-mobile channel are as predictable as the fixed to mobile channels in time. Compared with the derived bound, the performance of the algorithm approaches the bound as the SNR increases. Future work will evaluate the performance of mobile to mobile wireless channel predictors using real world measured data and in terms of communication and information theoretic system criterion.

References:

[1] A. S. Akki and F. Haber, "A statistical model of mobile-to-mobile land communication channel," *IEEE Transactions on Vehicular Technology*, vol. 35, pp. 2–7, 1986.

[2] A. S. Akki, "Statistical properties of mobile-to-mobile land communication channels," *IEEE Transactions on Vehicular Technology*, vol. 43, pp. 826–831, 1994.

[3] F. Vatalaro and A. Forcella, "Doppler spectrum in mobile-to-mobile communications in the presence of three-dimensional multipath scattering," *IEEE Transactions on Vehicular Technology,*, vol. 46, no. 1, pp. 213–219, 1997.

[4] A. Duel-Hallen, "Fading Channel Prediction for Mobile Radio Adaptive Transmission Systems," *Proceedings of the IEEE*, vol. 95, pp. 2299–2313, 2007.

[5] A. Duel-Hallen, S. Hu, and H. Hallen, "Long Range Prediction of Fading Signals: Enabling Adaptive

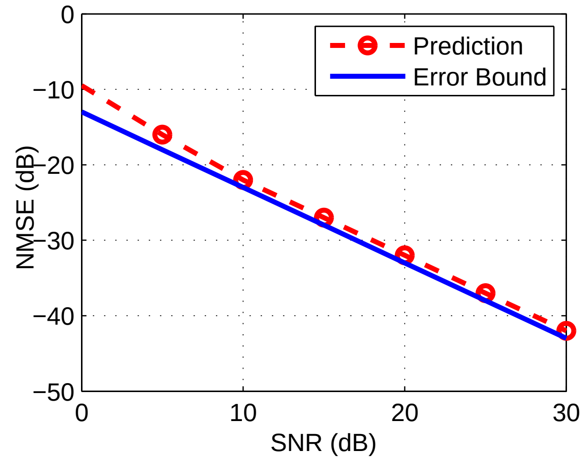

Figure 7: Prediction NMSE and error bound versus SNR for a prediction horizon of $50\,ms$ with 100 samples in the observation segment.

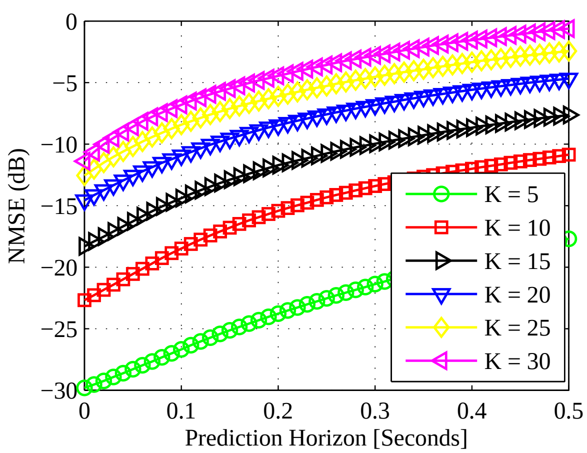

Figure 5: NMSE versus prediction horizon with different number of propagation paths at $\text{SNR} = 10\,dB$.

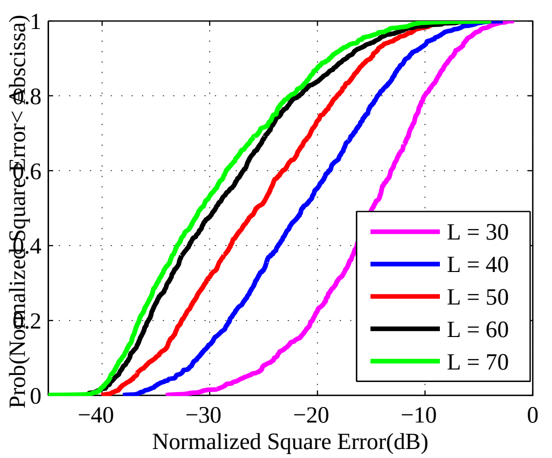

Figure 6: The CDF of prediction NSE for a prediction horizon of $100\,ms$ at $\text{SNR} = 10\,\text{dB}$ with different number of samples in the training segment.

Transmission for Mobile Radio Channels," *IEEE Signal Processing Magazine*, vol. 17, pp. 62–75, 2000.

[6] M. Chen and M. Viberg, "Long-range channel prediction based on nonstationary parametric modeling," *Trans. Sig. Proc.*, vol. 57, no. 2, pp. 622–634, Feb 2009.

[7] R. Adeogun, "Multipath Parameter Estimation and Channel Prediction for Wideband Mobile to Mobile Wireless Channel," *WSEAS Transactions on Communications*, vol. 13, pp. 201–208, April 2014.

[8] T. Ekman, "Prediction of Mobile Radio Channels - Modeling and Design," Ph.D. dissertation, 2002.

[9] P. Teal and R. Vaughan, "Simulation and performance bounds for real-time prediction of the mobile multipath channel," in *IEEE Workshop on Statistical Signal Processing Proceedings*, 2001, pp. 548–551.

[10] M. Chen, T. Ekman, and M. Viberg, "New approaches for channel prediction based on sinusoidal modeling," *EURASIP J. Appl. Signal Process.*, vol. 2007, no. 1, pp. 197–197, Jan 2007.

[11] J. Andersen, J. Jensen, S. Jensen, and F. Frederisen, "Prediction of future fading based on past measurements," in *IEEE VTC*, vol. 1, 1999, pp. 151–155.

[12] L. Huang, T. Long, E. Mao, H. C. So, and S. Member, "MMSE-Based MDL Method for Accurate Source Number Estimation," *IEEE Signal Processing Letters*, vol. 16, no. 9, pp. 798–801, 2009.

[13] M. Wax and T. Kailath, "Detection of signals by information theoretic criteria," *IEEE Transactions on Acoustics, Speech and Signal Processing*, vol. 33, no. 2, pp. 387–392, 1985.

[14] R. Roy and T. Kailath, "Signal processing part II," F. A. Grünbaum, J. W. Helton, and P. Khargonekar, Eds. New York, NY, USA: Springer-Verlag New York, Inc., 1990, ch. ESPRIT-estimation of signal parameters via rotational invariance techniques, pp. 369–411.

[15] S. M. Kay, *Fundamentals of statistical signal processing: estimation theory*. Upper Saddle River, NJ, USA: Prentice-Hall, Inc., 1993.